

## RESTORING FORCE CHARACTERISTICS AND DYNAMIC BEHAVIOR OF RC FRAME STRUCTURE BEFORE AND AFTER REPAIR OF THE DAMAGED BEAM END

S.NOMURA and H.KINUGASA and S.KAWATO

Department of Architecture, Science Univ. of Tokyo  
Yamazaki 2641, Noda city, Chiba, JAPAN

### ABSTRACT

This paper deals with the dynamic behavior of the ductile RC frame structure before and after repair of the damaged beam end on the basis of the following test results. To investigate the difference of hysteretic behavior by the combination of repair grade and residual angle correction, the following repairs to each specimen were made and tested : (A) No repair and no angle correction (Model A), (B) Repair of damaged end with no angle correction (Model B), (C) Repair of damaged end with angle correction (Model C).

### KEYWORDS

Repair; ductile RC frame; earthquake response analysis; residual deformation angle; P- $\delta$  effects; multi mass system.

### 1. INTRODUCTION

In the design of ductile frame structure which is based on plastic hinges at beam end, a certain degree of damage is allowed to strong earthquake motions. Then, the structure is expected to be repaired for further use after the damage. To investigate the dynamic behavior of those repaired RC frame structures, it is necessary first of all to know the restoring force characteristics of repaired beam members.

This paper is composed of the tests on repaired members after damage in attention with the correction of residual displacement, and the earthquake response analysis to the buildings where the restoring force characteristics are modeled by the test results.

### 2. REPAIRING OF DAMAGED BEAM AND ITS RESTORING FORCE CHARACTERISTICS

#### 2.1 REPAIRING AND TESTING PROCEDURE

To compare the difference of restoring force characteristics in repairing procedure, three same specimens were tested. The bar arrangement of the specimens is shown in Fig. 1, and the material properties are

shown in Table. 1, 2, and 3. The loading hysteresis is the reversed cyclic loading as shown in Fig. 2. The maximum angle of the last cycle is 32/1000 rad., which is five times as large as calculated yield displacement (6.4/1000 rad.). The axial load is 0, since these specimens are assumed to be beams.

[FIRST STAGE TEST]

All specimens were tested according to the cyclic loading program, where the maximum angle of the last cycle was 32/1000 rad. and the specimen was unloaded to no loading level where residual angle existed (Original Model).

[REPAIR AND SECOND STAGE TEST]

Each specimen was repaired by each method as shown in Fig. 3. Specimen A was reloaded from the last point of the first stage test with no repair works (Model A). The specimen B was repaired after experienced the first stage test at the damaged end (0 ~ 0.75D from the end) by casting new expansive mortar after chipping the damaged concrete. Fig. 4 shows the chipping part and repairing part of specimen B and C. Then specimen B was reloaded according to the same loading program (Model B). The specimen C was repaired after experienced the first stage test in the same way as specimen B, but the residual deformation angle was corrected to 0-degree before the repairing (Model C).

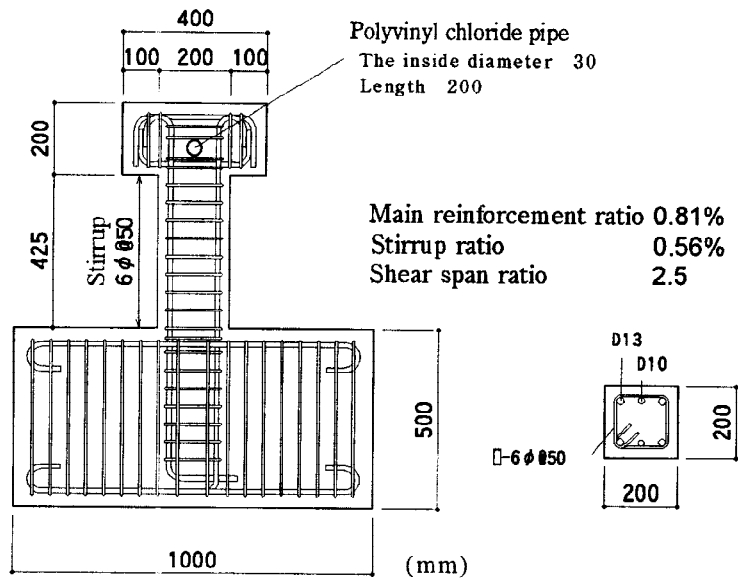


Figure 1. Bar arrangement drawing of specimen

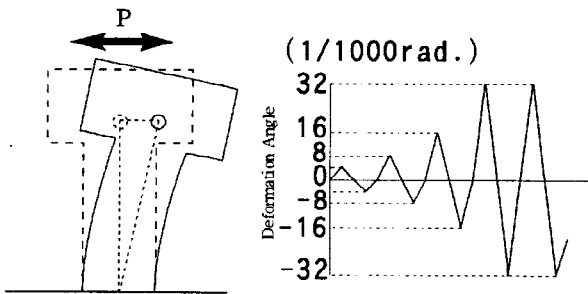


Figure 2. Loading hysteresis

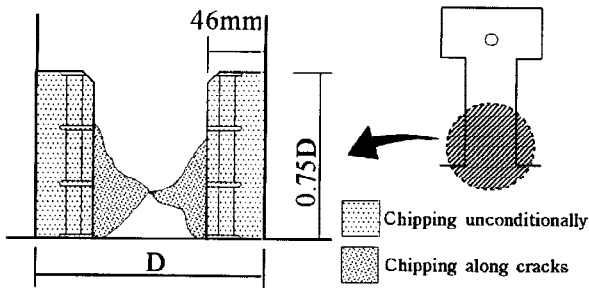


Figure 4. Chipping part

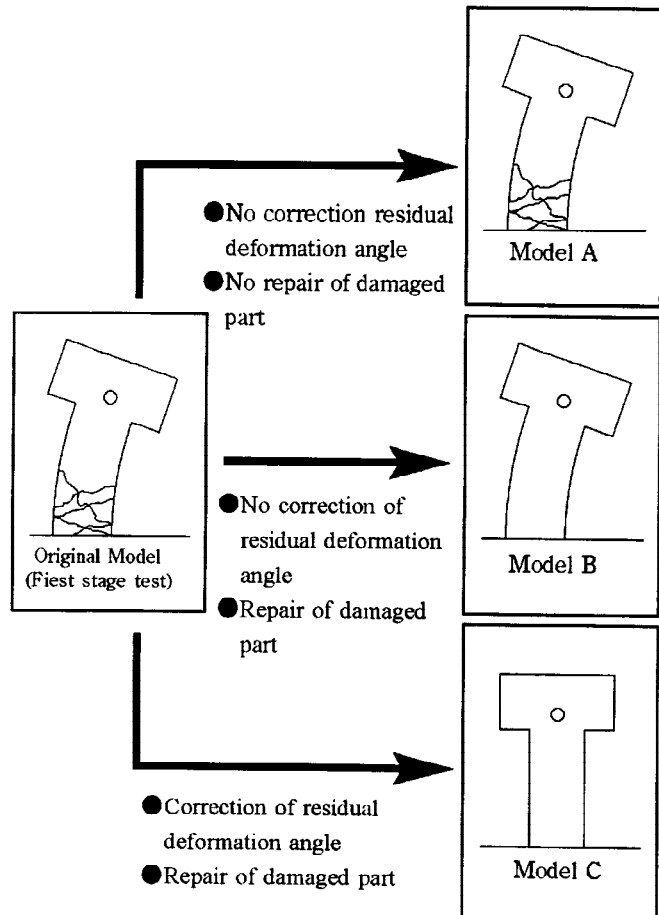


Figure 3. Repairing method of each model

Table 1. The material properties of main reinforcement

	Yield stress (kgf/cm <sup>2</sup> )	Tensile strength	Young's modulus	Sectional area (cm <sup>2</sup> )
6φ	3286	4329	1.895 × 10	0.280
D10	4358	5466	1.927 × 10	0.617
D13	3912	5254	1.982 × 10	1.105

Table 2. The material properties of concrete

Model	Strength(kgf/cm <sup>2</sup> )		Young's modulus (kg/cm <sup>2</sup> )
	compress	tension	
Model	356	32.5	2.63 × 10 <sup>5</sup>
Model	267	22.5	2.30 × 10 <sup>5</sup>
Model	267	22.5	2.30 × 10 <sup>5</sup>

Table 3. The material properties of expansive mortar for repairing

Model	Strength(kgf/cm <sup>2</sup> )		Young's modulus (kg/cm <sup>2</sup> )
	compress	tension	
Model	512	33.4	2.29 × 10 <sup>5</sup>
Model	545	33.4	2.42 × 10 <sup>5</sup>

## 2.2 RESTORING FORCE CHARACTERISTICS OF SPECIMENS BEFORE AND AFTER REPAIRING

### (1) FAILURE CHARACTERISTICS

Fig. 5 shows the crack distribution after loading test. On the Original Model and Model A, some remarkable shear cracks were observed. In case of Model A, new transverse tensile cracks developed at the lower part of the beam, and large amount of concrete peeled off. No new shear cracks developed, though transverse tension cracks grew and some new cracks developed. After all, the failure mode of Model A was not brittle but ductile. On the other hand, failure characteristics of Model B is similar to Model C and they were different from Model A. The damage of lower part was slight compared with Model A, because of the repairing with expansive mortar. But comparing Model B and Model C with Original Model, shear cracks of Model B and C grew and the crack width is wide. Besides concrete was peeled off at the joint of concrete and expansive mortar, and new shear cracks developed upward. Thus it is said that the failure mode of Model B and Model C is close to shear failure.

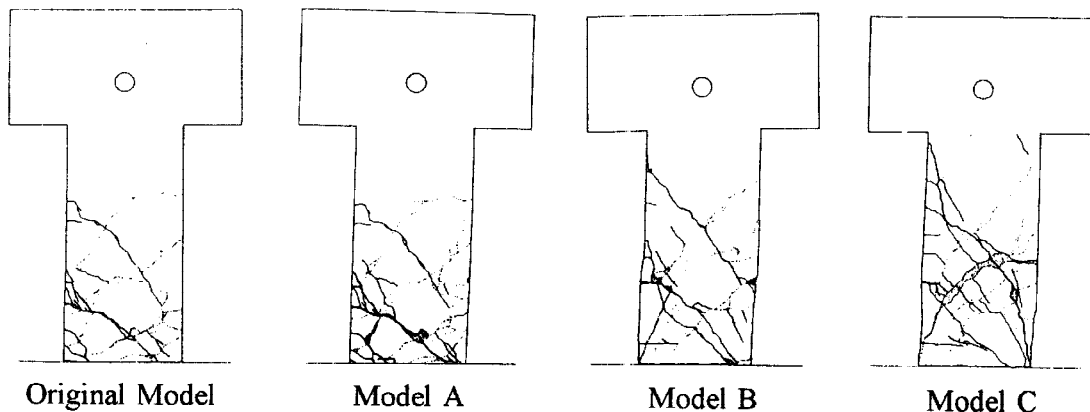


Figure 5. Crack distribution

### (2) LOAD-DEFORMATION ANGLE RELATIONSHIP

Fig. 6 shows the load - deformation curves of Model A, B, and C including those of Original Model. As shown in Fig. 6(a), the hysteresis curve of Model A exceed the maximum points of Original Model and it can be modeled as the continued curve of Original Model. In case of Model B and Model C as shown in Fig. 6(b) and (c), there was an increase of 15% or 20% in strength and a reduction in initial stiffness

and cracking load. The hysteresis loop of Model B has its central point at the point of residual deformation of Original Model. Since the curve of Model C whose residual deformation angle was corrected to a center of hysteresis loop of Original Model, it moves round the center of hysteresis loop of Original Model.

### (3) EQUIVALENT VISCOUS DAMPING RATIO

The relation of equivalent viscous damping ratio to load cycle is shown in Fig. 7. The equivalent viscous damping ratio of Model A is the smallest of those of the other models. Because, Model A was not repaired and most of the curves are in the already experienced crack region where little energy dissipation is expected. Model B and Model C show a reduction of viscous damping ratio about 20% at 4th cycle and about 40% at 5th cycle compared with Original Model.

### (4) RIGIDITY AND A RATE OF RIGIDITY REDUCTION

Fig. 8 and Fig. 9 show the rigidity and the rate of rigidity reduction - loading cycle relationship, where rigidity is the value of maximum strength divided by the maximum displacement of each cycle, and the rate of rigidity reduction is the value of rigidity divided by the rigidity at yielding. In case of Model A, it is clear that the value of the rigidity is quite small, and the rigidity increases as deformation increases, which is different from that of the other models. But this is understandable from the characteristics of this model as mentioned before. In case of Model B and Model C, initial stiffness is lower than that of Original Model, but the rigidity lowers gradually after cracking and the rigidity is a little higher than that of Original Model after yielding.

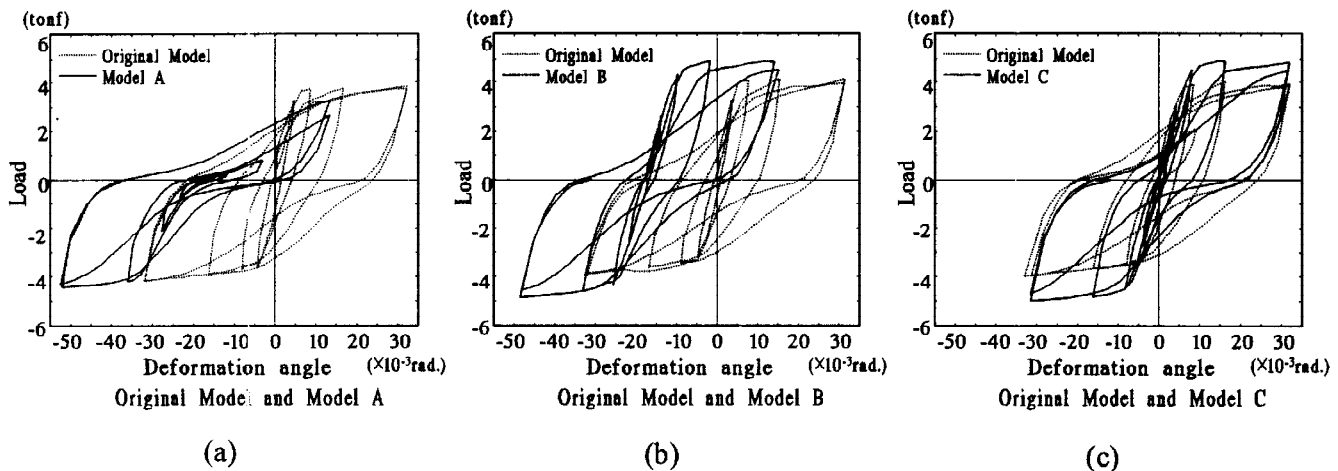


Figure 6. Load - deformation curve

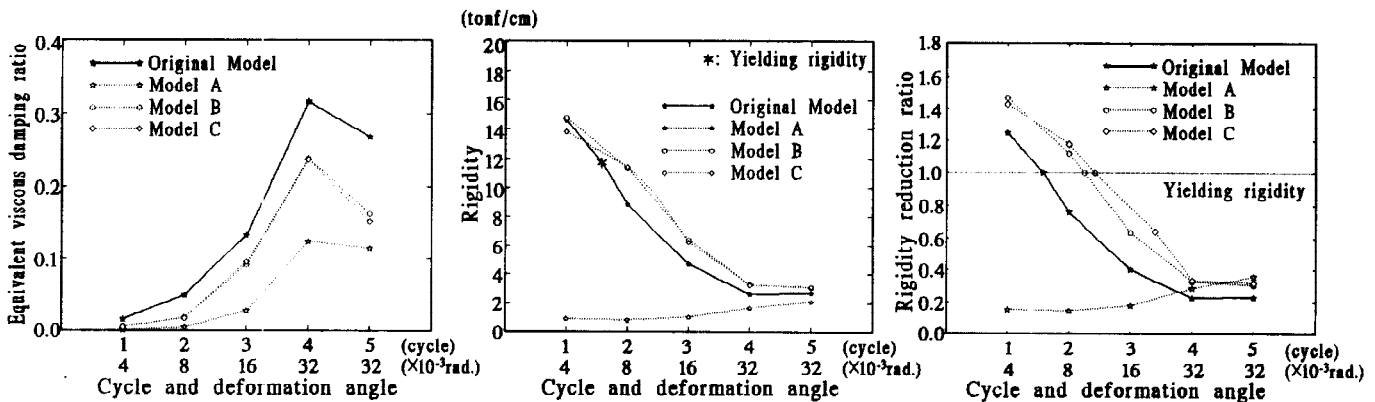


Figure 7. Equivalent viscous damping ratio

Figure 8. Rigidity

Figure 9. Rate of rigidity reduction

### 3. EARTHQUAKE RESPONSE ANALYSIS OF REPAIRED STRUCTURE

#### 3.1 ANALYTICAL MODEL

The five-story RC frame structure was taken as an analytical model for earthquake response and the restoring force characteristics of beam end was modeled based on experimental results. The analytical model was selected in a typical RC structures in Japan and modeled as shown in Fig. 10. Typical section of assumed model is shown in Fig. 11. The Newmark's  $\beta$  method ( $\beta=1/4$ ) was adopted as numerical integration method. The applied earthquake motions are EL-CENTRO 1940 NS and HACHINOHE 1968 EW that were increased by 1, 3, and 5 times.

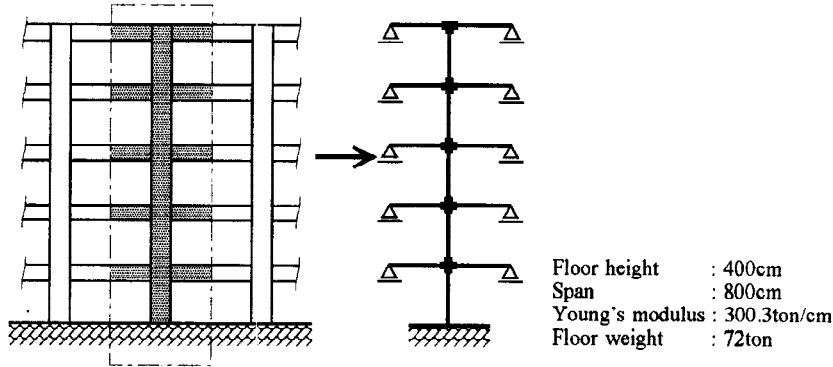


Figure 10. Analytical model

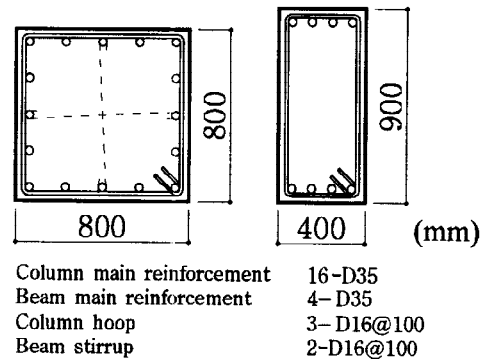


Figure 11. Typical section

Since the purpose of this study is to investigate the behavior of repaired structure, some of which have residual deformation. So it is important to consider the influence of gravity, namely, P- $\delta$  effect to analytical model. The P- $\delta$  effect is generally treated as a factor that cause rigidity reduction of a structure. In case of single mass system as shown in Fig. 12, that is

$$m\ddot{\delta} + c\dot{\delta} + \left(k - \frac{mg}{h}\right)\delta = -m\ddot{x}_0 \quad (1)$$

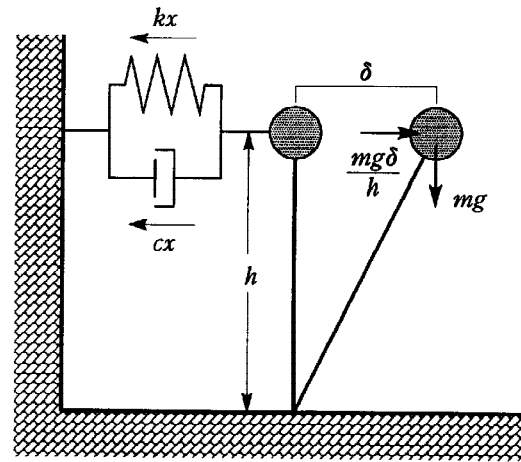


Figure 12. P- $\delta$  effect of single mass system

But in this study, the lateral load provided by the P- $\delta$  effect is treated as external force as follows to simplify the calculation of analysis.

$$m\ddot{\delta} + c\dot{\delta} + k\delta = -m\ddot{x}_0 + \frac{mg\delta}{h} \quad (2)$$

In case of the multi mass system, the lateral load that causes the same moment as the moment by gravity was assumed as external force by P- $\delta$  effect (see Fig.13). Therefore the lateral load of  $i$ th story of  $n$  storied structure  $f_i$  is

$$f_i = \frac{\sum_{j=i}^n mg\delta_j}{h_i} - \frac{\sum_{j=i+1}^n mg\delta_{j+1}}{h_{j+1}} \quad (i < n) \quad (3)$$

$$f_i = \frac{mg\delta_i}{h_i} \quad (i = n) \quad (4)$$

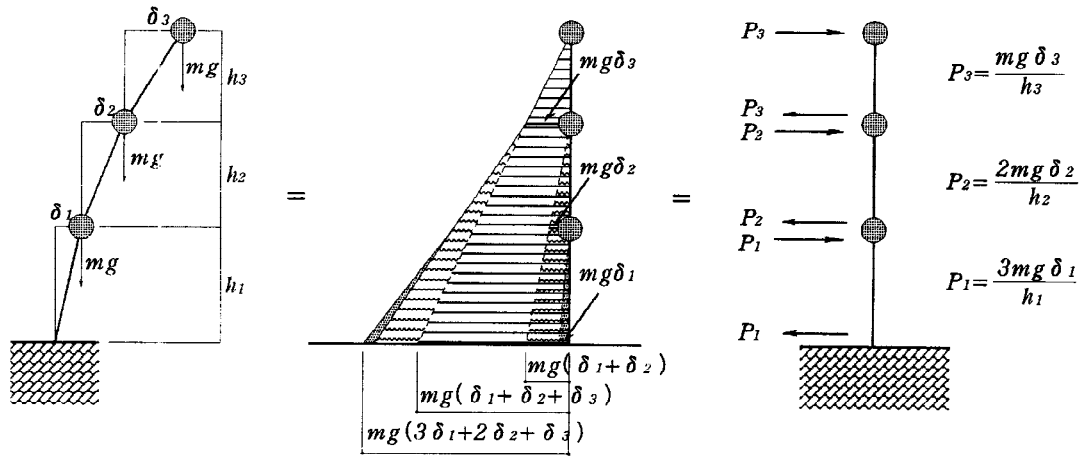


Figure 13. P- $\delta$  effect of multi mass system

### 3.2 MODELING OF MEMBERS

Each member and column is modeled by rigid plastic spring end method, where the beam-column joint are considered as rigid zone and every member is replaced by line members and rigid plastic spring is jointed to the end of rigid zone as shown in Fig. 14. The shear strain is assumed as elastic. In consideration of transverse tension cracks, the tri-linear type was adopted as the skeleton curve (moment - rotation angle relationship) of columns and beams as shown in Fig. 15(a). But it was assumed that columns

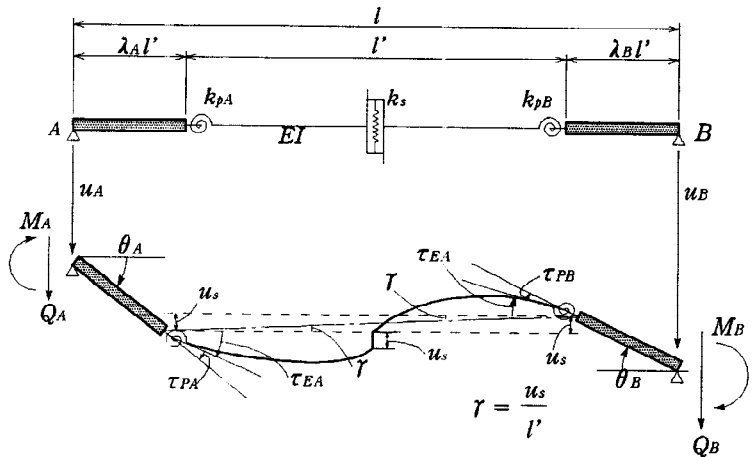


Figure 14. Rigid plastic spring end method

do not yield except the column base of first floor. In addition, the skeleton curve of Model B and Model C were assumed as shown in Fig. 15(b) on the basis of experimental results, namely, the strength was assumed to increase to 115 % of that of Original Model, and the cracking moment was assumed to decrease to 1/10 of that of Original Model. And in case of Model B, the starting point of hysteresis loop was moved to the point of the residual deformation. In case of Model A, the last response results of Original Model are considered as initial data and analyzed again. D.D.Tri model as shown in Fig. 16 was used for restoring force characteristics. Equivalent viscous damping ratio was set to agree with experimental results by multiplying unloading stiffness by coefficient  $a$  to coincide equivalent viscous damping ratio with observed value. The reduction rate of rigidity at yield point  $\alpha_y$  was assumed uniformly 0.3.

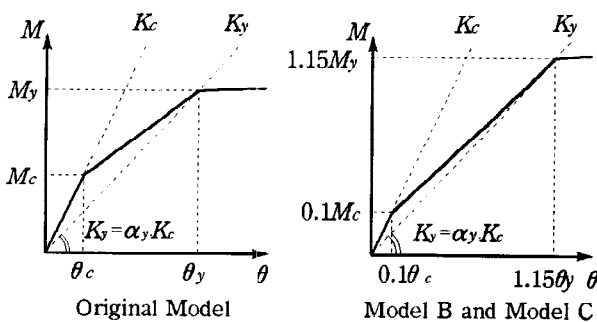


Figure 15. Skeleton curve

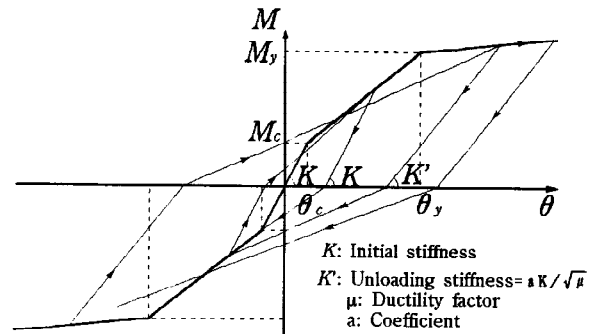


Figure 16. D.D.Tri model

### 3.3 RESPONSE OF REPAIRED MODELS

Since the response analysis results shows approximately the same tendency regardless of the magnitude and kind of earthquake motion, the results which obtained by using EL-CENTRO 1940 NS that increased by 5 times are shown below on behalf of response analysis results.

#### (1) Model A and Model B

Fig. 17.(a) shows the time - deformation angle relationship of Model A and Model B. Though both curves start from the point of residual deformation angle of Original Model, that of Model A gets close to the curve of Original Model and moves on almost the same curve as Original Model. Model A shows mostly the same maximum displacement as that of Original Model, but the residual displacement is larger. On the other hand, the curve of Model B looks like parallel to the curve of Original Model in the direction that residual displacement appeared. This is because that the center of hysteresis loop moved to the point of residual displacement by repairing with no residual deformation angle correction. Thus both maximum deformation angle and residual deformation angle of Model B are much larger than Original Model. So in this case, it is considered that Model B which was repaired with no deformation angle correction is more dangerous than Model A which was not repaired and whose residual deformation angle was not corrected.

#### (2) Model A and Model C

Fig. 17.(b) shows the time - deformation angle relationship of Model A and Model C. It is clear that though almost no difference occurs in maximum response, the residual deformation of Model C is much smaller than that of Model A and Original Model. It is considered that the action directed toward the center of hysteresis loop grow strong by the decrease of the unloading stiffness when the restoring force characteristics modeled. It is clear that the repairing method of Model C is the safest in the repairing methods tested in this study. But in practice, to correct residual deformation angle is usually expensive with some difficulties. In addition, though shear strain was treated as elasticity in this study, there is a possibility of shear failure by the increase of bending strength.

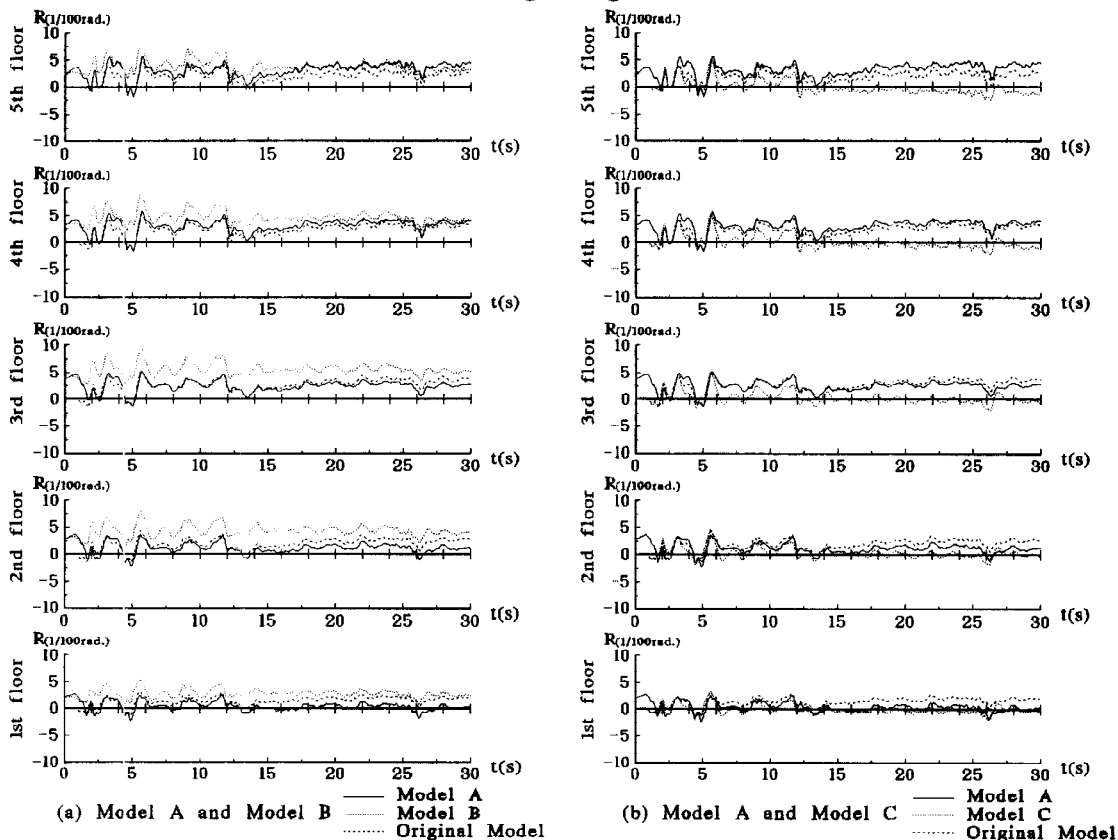


Figure 17. Time - deformation angle relationship

### (3) P- $\delta$ effect

Fig. 18. shows the time - deformation angle relationship comparing P- $\delta$  effect on earthquake response. In case of Original Model (Fig. 18(a)), though almost no difference is shown in maximum response, the residual displacement of the curve considering P- $\delta$  effect is much larger than the other. But in case of Model C (Fig. 18(b)), the two curves show almost the same behavior, and the residual displacement is sometimes smaller than that of Original Model. This is considered as the effect of a decrease of unloading stiffness as described above.

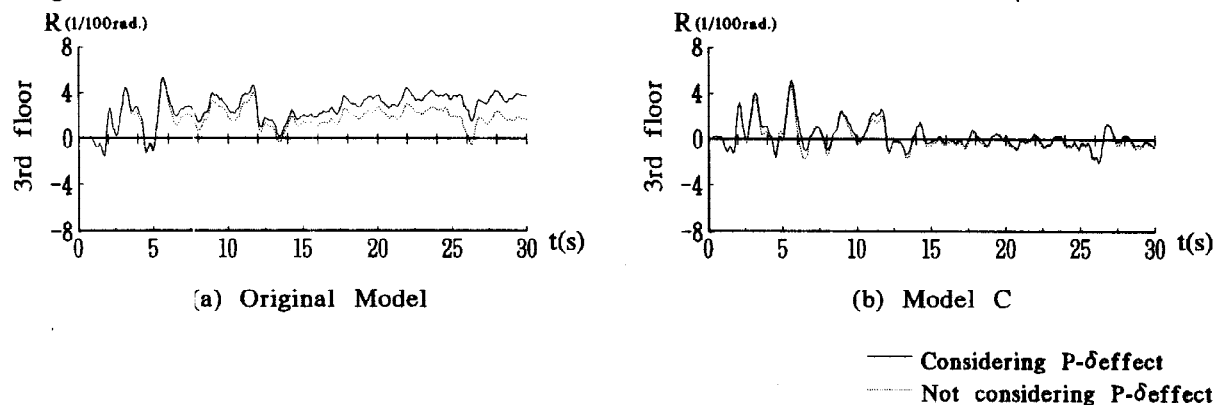


Figure 18. The influence of P- $\delta$  effect

## 4. CONCLUSION

From the test results,

- The repaired models (Model B and Model C) have the tendency of less initial rigidity, less hysteretic energy dissipation, but higher yielding strength, compared with Original model.
- Model B behaves almost the same as Original Model by shifting the origin point to the residual deflection point.

From the earthquake response analysis,

- Both the maximum displacement and the residual displacement of Model B are higher than those of Original Model.
- Model A shows almost the same maximum displacement as that of Original Model, but the residual displacement are sometimes larger.
- Because of the decrease of the unloading stiffness when the restoring force characteristics was modeled, Model C shows less maximum displacement than those of Original Model.
- The P- $\delta$  effect on residual deformation is large, though that on the maximum displacement is negligible small.

## REFERENCES

- Sogabe, H., Odaka, T. (1994). *P- $\delta$  effect on elasto-plastic response of lumped mass system subjected to strong-motion earthquakes*. Architectural Institute of Japan No.463: 19-26
- Shibata, A. (19 ). *The newest structural analysis*. Morikita publication
- Morihama, K., Kobayashi, S. (1984). *Repairing effect of RC column member subjected to an earthquake disaster*. JCI 6th Conference: 621-624